AD_____

Award Number:
W81XWH-11-1-0172

TITLE:
Oxidative Stress Increases the Blood Brain Barrier Permeability Resulting in Increased Incidence of Brain Metastasis in BRCA Mutation Carriers

PRINCIPAL INVESTIGATOR:

Hava Avraham, Ph.D.

CONTRACTING ORGANIZATION: Beth Israel Deaconess Medical Center
Boston, MA 02215-5491

REPORT DATE: August 2014

TYPE OF REPORT: Final

PREPARED FOR: U.S. Army Medical Research and Materiel Command
Fort Detrick, Maryland 21702-5012

DISTRIBUTION STATEMENT:
Approved for Public Release; Distribution Unlimited

The views, opinions and/or findings contained in this report are those of the author(s) and should not be construed as an official Department of the Army position, policy or decision unless so designated by other documentation.

REPORT DOCUMENTATION PAGE

Form Approved
OMB No. 0704-0188

Public reporting burden for this collection of information is estimated to average 1 hour per response, including the time for reviewing instructions, searching existing data sources, gathering and maintaining the data needed, and completing and reviewing this collection of information. Send comments regarding this burden estimate or any other aspect of this collection of information, including suggestions for reducing this burden to Department of Defense, Washington Headquarters Services, Directorate for Information Operations and Reports (0704-0188), 1215 Jefferson Davis Highway, Suite 1204, Arlington, VA 22202-4302. Respondents should be aware that notwithstanding any other provision of law, no person shall be subject to any penalty for failing to comply with a collection of information if it does not display a currently valid OMB control number. **PLEASE DO NOT RETURN YOUR FORM TO THE ABOVE ADDRESS.**

1. REPORT DATE	2. REPORT TYPE	3. DATES COVERED
August 2014	Final	24Jan2011-23Jan2014

4. TITLE AND SUBTITLE
Oxidative Stress Increases the Blood Brain Barrier Permeability Resulting in Increased Incidence of Brain Metastasis in BRCA Mutation Carriers

5a. CONTRACT NUMBER

5b. GRANT NUMBER
W81XWH-11-1-0172

5c. PROGRAM ELEMENT NUMBER

6. AUTHOR(S)
Hava Avraham, Ph.D (original report)
Revised report prepared by Vikas P. Sukhatme, MD ScD

Email: vsukhatm@bidmc.harvard.edu

5d. PROJECT NUMBER

5e. TASK NUMBER

5f. WORK UNIT NUMBER

7. PERFORMING ORGANIZATION NAME(S) AND ADDRESS(ES)
Beth Israel Deaconess Medical Center
Boston, MA 02215-5491

8. PERFORMING ORGANIZATION REPORT NUMBER

9. SPONSORING / MONITORING AGENCY NAME(S) AND ADDRESS(ES)
U.S. Army Medical Research and Materiel Command
Fort Detrick, Maryland 21702-5012

10. SPONSOR/MONITOR'S ACRONYM(S)

11. SPONSOR/MONITOR'S REPORT NUMBER(S)

12. DISTRIBUTION / AVAILABILITY STATEMENT
Approved for Public Release; Distribution Unlimited

13. SUPPLEMENTARY NOTES

14. ABSTRACT
BRCA1 is a multifunctional tumor suppressive protein. Knockout of wt BRCAI in breast cancer cells resulted in an increase in cell proliferation, anchorage-independent growth, cell migration, invasion and a loss of p21/Wafl and p27Kipl expression. Further, in BRCAI knocked-down cells, the expression of survivin was significantly up-regulated with a decrease in cellular sensitivity to paclitaxel. Cells that harbor endogenous mutant or defective BRCA l (such as MDA-MB-436 and HCC1937) were highly proliferative and expressed a relatively low levels of p21/Wafl and p27Kip I and high level of survivin and were resistant to paclitaxel. Thus, mutated BRCAI or loss of wt BRCA1 up-regulates the malignant cell behavior. However, it is still not clear how tumor cells expressing mutant BRCAI have enhance tumorigenicity in vivo.

15. SUBJECT TERMS- Breast Cancer

16. SECURITY CLASSIFICATION OF:			17. LIMITATION OF ABSTRACT	18. NUMBER OF PAGES	19a. NAME OF RESPONSIBLE PERSON
a. REPORT	b. ABSTRACT	c. THIS PAGE			USAMRMC
U	U	U	UU	18	19b. TELEPHONE NUMBER *(include area code)*

Table of Contents

FINAL REPORT

I. INTRODUCTION

BRCA1 is a multifunctional tumor suppressive protein. Knockout of wt BRCAI in breast cancer cells resulted in an increase in cell proliferation, anchorage-independent growth, cell migration, invasion and a loss of p21/Wafl and p27Kipl expression. Further, in BRCAI knocked-down cells, the expression of survivin was significantly up-regulated with a decrease in cellular sensitivity to paclitaxel. Cells that harbor endogenous mutant or defective BRCA l (such as MDA-MB-436 and HCC1937) were highly proliferative and expressed a relatively low levels of p21/Wafl and p27Kip I and high level of survivin and were resistant to paclitaxel. Thus, mutated BRCAI or loss of wt BRCA1 up-regulates the malignant cell behavior. However, it is still not clear how tumor cells expressing mutant BRCAI have enhance tumorigenicity *in vivo*.

II. HYPOTHESIS

We hypothesize that adhesion of BRCA I mutated cells to endothelial cells activates several distinct signaling pathways to induce MMP gene expression and increased ROS levels. We hypothesize that oxidative stress induced by adhesion of cells with mutated BRCA1 to HBMEC results in alterations in the integrity of the blood-brain barrier (BBB) and changes of the tight-junctions, leading to transmigration of tumor cells across the BBB and colonization of these cells in the brain forming breast cancer metastasis in the brain.

Specific Aims

1) Elucidate the molecular mechanisms and signaling pathways by which adhesion of breast cancer cells expressing mutated BRCA1, as compared to breast cancer cells expressing wt BRCA1, induces reactive oxygen species (ROS) production in human brain microvascular endothelial cells.
2) Examine the effects of oxidative stress on tight junction expression (ZO-1, ZO-2, occludin and claudin-5), permeability and integrity of the brain endothelium using *in vitro* and *in vivo* models.
3) Determine the protective effects of PARP inhibitors and/or selenium in preventing BBB-induced damage by oxidative stress, and in inhibiting breast cancer metastasis to the brain.

Further, since selenium has anti-cancer properties that are linked with protection against oxidative stress and Poly (ADP-ribose) polymerase (PARP) inhibitors have shown activity against BRCA1 and BRCA2 deficient cancers, we will therefore analyze their therapeutic potential to inhibit damage to the BBB and transmigration of tumor cells across the BBB.

III. SUMMARY OF RESULTS

Year 1

Aims

1) Elucidate the molecular mechanisms and signaling pathways by which adhesion of breast cancer cells expressing mutated BRCA1, as compared to breast cancer cells expressing wt BRCA1, induces reactive oxygen species (ROS) production in human brain microvascular endothelial cells.

Results

Cocultures of HBMEC and human astrocytes as an in-vitro human blood-brain barrier model: The astrocyte- endothelial cocultures were established as a BBB model system using the transwell coculture system (Corning Costar, Cambridge, MA). Briefly, HBMEC were grown to confluence in 12-well plastic tissue culture plates, after which the culture medium was changed to media containing 10% FCS.

Concurrently, astrocytes were grown to confluence on semiporous 0.45 nm transwell inserts. Cocultures were initiated by transferring inserts containing astrocytes directly into wells containing confluent HBMEC. After 48 h incubation, endothelial cells were collected for further analysis. These cocultures were also tested for the maintenance of a tight endothelial permeability barrier by determination of the paracellular permeability of the BBB monolayers for ^{3}H-inulin and ^{14}C-sucrose.

Effects of ROS on permeability changes in HBMEC: To examine if oxidative stress induced by adhesion of HCC1937 cells to HBMEC could be the cause of HBMEC impairment, we examined the effects of ROS on HBMEC in cocultures of breast cancer cells with HBMEC using the DCF-DA fluorescence assay. H(2)O(2) (100µM), a ROS-donating agent was used as positive control. Adhesion of HCC1937 to HBMEC showed increase in ROS levels as compared to control, and this increased in ROS formation was abrogated by the antioxidant uric acid, UA (Table 1).

Table 1: Adhesion of HCC1937 cells induced oxidative stress on brain endothelial cells Adhesion of cells Fluorescence Intensity (x10^{3})/mg Protein in HBMEC

	No Treatment	UA
HCC1937	23 ± 4	17 ± 4
HCC1937/WT BRCA1	15 ± 3	14 ± 2
MCF-7	14 ± 3	12 ± 3
MCF-7/mutated BRCA1	22 ± 2	18 ± 4
Control PBS	6 ± 1	5 ± 3
H(2)O(2) /HBMEC	27 ±4	13 ± 2

Table 1: Cultures of breast cancer cells with either untreated or pretreated with the antioxidant UA (50µM). As positive control, HBMEC were treated with ROS donors for 2 hours H(2)O(2). The breast cancer cells were then added to HBMEC monolayers for adhesion. After 6 hours, the tumor cells were removed, and HBMEC monolayers were washed and ROS production in HBMEC was examined using the kit for detection of ROS based on DCF-Dais converted to highly fluorescent DCF by ROS. The fluorescence was detected at excitation 488 nm and at 525nm emission spectra using a florescence plate reader. Results were expressed as specific mean fluorescence intensity (MPI) per mg protein. Based on these results, the adhesion of HCC1937 with HBMEC induced ROS generation in HBMEC.

Next, we examined the effects of ROS on permeability changes of HBMEC. HBMEC integrity was analyzed by TEER and pattern of tumor cell migration across HBMEC. As shown in Table 2, significant increase in HBMEC permeability was observed by ROS and these changes were inhibited in the presence of UA antioxidant, uric acid, indicating the involvement of ROS in loss of the HBMEC integrity. The functional changes paralleled enhanced tumor cell migration across HBMEC (Table 2). Thus, we suggest that ROS induced adhesion of BRCA1 carrier cells to HBMEC resulted in modification of cytoskeleton organization and loss of HBMEC integrity and increased tumor migration across the HBMEC.

Table 2: Effects of ROS on TEER and cell migration across HBMEC

Cells:	Treatment	TEER of HBMEC (% of Control)	% Tumor cell migration across HBMEC
HCC1937:	No Treatment	82 ± 3*	22 ± 3*
	UA	96 ± 2	7 ± 2
HCC1937/WT BRCA1:	No Treatment	91 ± 4	13 ± 3*
	UA	94 ± 5	5± 1
HBMEC:	H(2)O(2)	82 ± 4*	18 ± 3*
	UA+ H(2)O(2)	96 ± 2	7 ± 4
	PBS	100%	0%

Table 2: TEER measurement across the HBMEC monolayer assessed the BBB tightness. TEER values recorded in ohms. Results are from two experiments in triplicate. Results were expressed as mean percent of controls. *p<0.05 as compared to HBMEC control. The transmigration of cells was assessed after 6 hours. The % of cell transmigrates out of the total input. *p<0.05 as compared to control.

Effects of ROS and PARP inhibitors on permeability of tumor cells across HBMEC

We analyzed the effects of these inhibitors on permeability of HBMECs by TEER assay. As shown in Table 3, the permeability of HBMEC was increased in the presence of HCC1937/MT cells, as compared to WT cells. Changes in permeability as analyzed by TEER were reduced in the presence of either COX-2, PARP or ROS inhibitors.

Cells	**Treatment**	**TEER of HBMEC (% of Control)**
HCC1937/MT BRCA1	-	83±3**
	ROS inhibitor	93±4
	PARP inhibitor	94±3
Cells	**Treatment**	**TEER of HBMEC (% of Control)**
HCC1937/WTBRCA1	-	90±3*
	ROS inhibitor	94±5
	PARP inhibitor	95±2
HBMECs	-	100

Table 3: Effects of ROS and PARP inhibitors on TEER. TEER values recorded in ohms. Results are from three experiments in triplicate. Results were expressed as mean percent of controls. *p<0.05 as compared to HBMEC control; **p<0.005 as compared to HBMEC control.

Year 2
Aims

2) Examine the effects of oxidative stress on HBMEC-tight junction expression (ZO-1 and claudin-5) *in vitro* and *in vivo*.
3) Determine the protective effects of PARP and ROS inhibitors, as well as COX-2 inhibitors in preventing BBB induced change and breast tumor colonization in brain.

Results

Since the BBB function is maintained by the presence of a continuous tight junction (TJ) complex, we investigated the effects of HCC1937 cells expressing mutant BRCA1, as compared to HCC1937/WT-BRCA1 expressing WT BRCA1 in HBMECs 3D cocultures of human astrocytes together with HBMEC system, on HBMEC-TJ integrity. While HBMECs expressed a linear and continuous distribution at cell-cell boundaries with normal ZO-1 and claudin-5 distribution (Fig. 1A), the cocultures of HCC1937 expressing mutant BRCA1 resulted in significantly damaged and less continuous, non-linear appearance in HBMECs or completely missing at several cell-cell boundaries (Fig. 1C). Interestingly, HCC1937/BRCA1 was capable of maintaining some TJ structures in HBMECs (Fig. 1B), and the damage of BMEC-TJs was less severe as compared to that of HCC1937.

The addition of ROS inhibitor or COX-2 inhibitor directly to HBMEC cultures was toxic and caused apoptosis of HBMEC at 50nM (Fig. 2A) or at 25nM (data not shown). In cocultures of HBMECs and HCC1937 (Fig. 3B) and HCC1937/WT-BRCA1 (Fig. 3A), ROS inhibitor by itself was unable to prevent damage of TJ structures in HBMECs (Fig. 3). However, ROS inhibitor showed some protective effects on HBMEC-TJs ZO-1 and claudin-5, as compared to cocultures with HCC1937 cells. Further, PARP inhibitor at 40μM was also toxic to HBMEC cocultures (Fig. 2B).

Since we observed some protective effect with HCC1937/WT-BRCA1, we examined the expression of TJ structures (ZO-1 and claudin-5) in the presence of HCC1937//WT-BRCA1 in more details. The presence of TJs ZO-1 and claudin-5 on HBMECs was less damaged (Fig. 4B) as compared to control HBMECs (Fig. 4A). Interestingly, these changes in TJs were minimized in the presence of COX-2 inhibitor (Fig. 4C). These data strongly suggest that mutated BRCA1 expressing tumor cells are more aggressive in causing damage to BMECs and the BBB. Interestingly, we observed that HCC1937 cells express high level of COX-2 by RT-PCR (Fig. 5A) and western blotting (Fig. 5B), while HCC1937/WT-BRCA1 had no expression of COX-2 (Fig. 5B). Thus, WT-BRCA1 inhibits COX-2 expression in tumor cells.

Next, we performed in vivo studies on the effects of MT-BRCA1 expressing tumor cells on the BBB integrity, TJ complexes in BMECs, and mammary tumor colonization in brain. Mice were injected with GFP-HCC-1937 or with GFP-HCC-1937/WT BRCA1 to the carotid artery (10^6 cells). After 7 weeks, the mice were euthanized and the BBB permeability in the brain of these mice was analyzed. As shown in Table 4, there were significant changes in the BBB in both groups. Neither inhibitors for ROS or PARP were able to prevent changes in the BBB integrity with both HCC1937 and HCC1937/WT although the changes were more dramatic with HCC1937 cells. Since COX-2 was more effective in vitro in preventing BBB permeability and TJ changes (Fig. 4C), we examined the potential of COX-2 inhibitor to inhibit BBB permeability

changes and tumor colonization in brain. We employed 4T1-BrM5 mammary epithelial cells that express MT-BRCA1 and injected them into the mammary fat pads of BALB/c mice. Within 2 weeks, tumor growth in the mammary fat pads was observed as shown in Table 5A. COX-2 inhibitor inhibited tumor growth in vivo in the mammary fat pads (note different scale between panels A and B in Table 5). Further, COX-2 inhibitor decreased BBB permeability (10 mice per group per treatment), as analyzed by Evans blue test (data not shown). Further, in vivo imaging of the brain samples from these mice showed reduced colonization of 4T1-BrM5 tumor cells in brain by COX-2 inhibitor (1 out of 10 mice had tumor colonization in brain, Fig. 6B) as compared to brain tumor colonization without treatment (10 out of 10 mice had tumor colonization in brain, Fig. 6A). Further, while tumor colonization of 4T1BrM5 was observed on day 10 (Fig. 6A) in Balb/c brain, we were able to observe tumor colonization in one mouse treated with COX-2 inhibitor only after 5 weeks (Fig. 6B).

Figure and Table Legends

Figure 1: BRCA1 mutant expressing cells induced changes in the distribution of ZO-1 and claudin-5 TJ proteins in HBMECs

3D cocultures of HBMECs with human astrocytes were either cocultured in the presence of HCC 1937 expressing MT BRCA1 (HCC MT) or wild type BRCA1 (HCC WT) for 6 hours and fixed immediately with 2% paraformaldehyde. Cells were then probed for ZO-1 and claudin-5 expression and visualized by indirect immunoflorescence using Alex Fluor 568 (red) conjugated secondary antibody (Molecular Probes). Nuclei were counterstained with DAPI (blue). Arrowheads indicated intact claudin-5 and ZO-1 TJs as indicated. Images shown are from a representative axial plane and are representative of over 30 fields examined in at least three independent experiments. Scale bar = 20 μm.

Figure 2: Effects of COX-2 inhibitor and ROS inhibitor of BMEC-TJs

HBMEC cocultures were preincubated with PARP inhibitor (30mM) or with ROS inhibitor (10mM selenium) for 6 hours. Immunostaining of TJs ZO-1 and claudin-5 was performed as described in Fig. 1.

Figure 3: Effects of ROS inhibitor on BMEC-TJs in the presence of HCC 1937 cells expressing mutant BRCA1 or WT BRCA1

HBMEC cocultures were pretreated with ROS inhibitor (50mM) for 1 hour. HCC-MT/BRCA1 or HCC-WT/BRCA1 cells were then added to HBMEC cocultures for 6 hours. The immunostaining of ZO-1 and claudin-5 TJs on BMECs were performed as described in Fig. 1.

Figure 4: Effects of HCC-BRCA1/WT and COX-2 inhibitor in vitro on BMEC-TJs

3D cocultures of HBMECs with human astrocytes were established and cocultured with HCC 1937 cells expressing WT BRCA1 in the absence of presence of COX-2 inhibitor (30 mM COX-2 inhibitor celecoxib). TJs immunostaining of ZO-1 and claudin-5 were performed as detailed in Fig. 1.

Figure 5: Expression of COX-2 in HCC1937 and HCC1937/WT-BRCA1 by RT-PCR (Panel A) and Western blotting (Panel B)

A. For RT-PCR, we obtained mRNA from both cell lines. RNA concentration was 0.211 μg/μl for HCC1973 and 0.264 μg/μl for MCF-7. RT-PCR analysis was run with 158 bp primer (Zattelli et al.) at annealing temperature of 52 °C using Qiagen One step RT-PCR kit was used for

the analysis.
B. Western blot analysis using COX-2 antibody from Santa Cruz (cat#sc-19999, lot F0510 product) with 72 kd.

Figure 6: Internal images of murine mammary epithelial tumor (4T1BrM5-GFP) metastasis in brain
Murine breast metastasis in the mouse brain was imaged by GFP expression. Images show metastatic lesions in the brain.
A. Series of internal fluorescence images of metastatic lesions in the brain in mice administered with 4T1BrM5-GFP mammary tumor cells into mammary fat pads at day 10 or 17 as compared to WT control brain (C1, C2)
B. Series of internal fluorescence images of metastatic lesions in the brain in mice administered with 4T1BrM5-GFP cells and COX-2 inhibitor taken at week 5 following treatment. The GFP positive signal in the mammary tumor is shown as a positive control.

Table 4: Quantitative analysis of TJs in vivo in brain: The changes in BBB TJs were analyzed 7 weeks following administration of HCC 1937/MT (HCC/MT) - BRCA1 or HCC 1937/WT(HCC/WT)-BRCA1 cells in the absence or presence of ROS inhibitor selenium (5mg/kg) or PARP inhibitor AZ0228 (10mg/kg) i.v. one hour before tumor cell injection. Quantification of CD31 positive BMEC expression and TJ proteins claudin-5 and ZO-1 (n=12, random sections, 10 mice per group) was performed. The TJs of the samples were analyzed, quantitated and compared to control brain. The TJs in control brain were defined as 100%. Percent changes in treated samples, as compared with control brain were calculated. Data are presented as mean +/- 1:SD *$p < 0.05$, **$p < 0.005$.

Table 5: BALB/c mice were administered either vehicle control (Panel A) or COX-2 inhibitor celecoxib at 10 mg/kg (Panel B), one hour before injection of 4T1-BrM5 tumor cells (100,000 cells) into the mammary fat pads (10 mice per group per treatment). Live mice were then sacrificed at day 21 and tumor volume in the mammary fat pads was measured. Some of the mice died during the experiment. Therefore, we have no data for those mice, as indicated.

Treatment	Quantification of TJ change (%)	
	ZO-1	Claudin-5
WT-control brain	100%	100%
HCC/MT BRCA1 + vehicle control	42 ± 8**	22 ± 7*
HCC/MT BRCA1 + ROS inhibitor	37 ± 11**	17 ± 6*
HCC/MT BRCA1 + PARP inhibitor	41 ± 14**	26 ± 7*
HCC/WT BRCA1 + vehicle control	28 ± 9**	21 ± 11*
HCC/WT BRCA1 + ROS inhibitor	30 ± 8**	20 ± 7*
HCC/WT BRCA1 + PARP inhibitor	27 ± 8**	19 ± 8*

TABLE 4

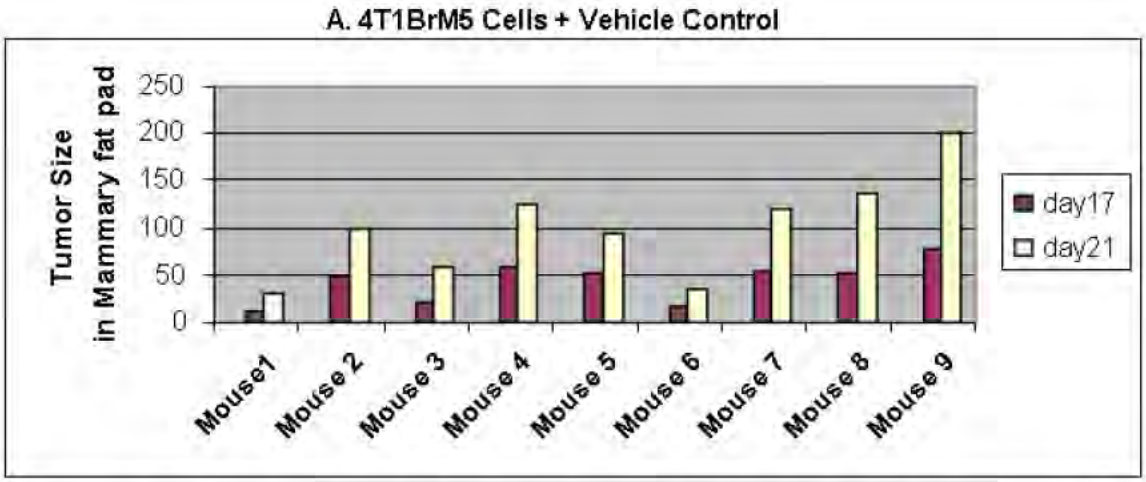
A. 4T1BrM5 Cells + Vehicle Control
Tumor Size in Mammary fat pad
250
200
150
100
50
0
Mouse1
Mouse 2
Mouse 3
Mouse 4
Mouse 5
Mouse 6
Mouse 7
Mouse 8
Mouse 9
day17
day21

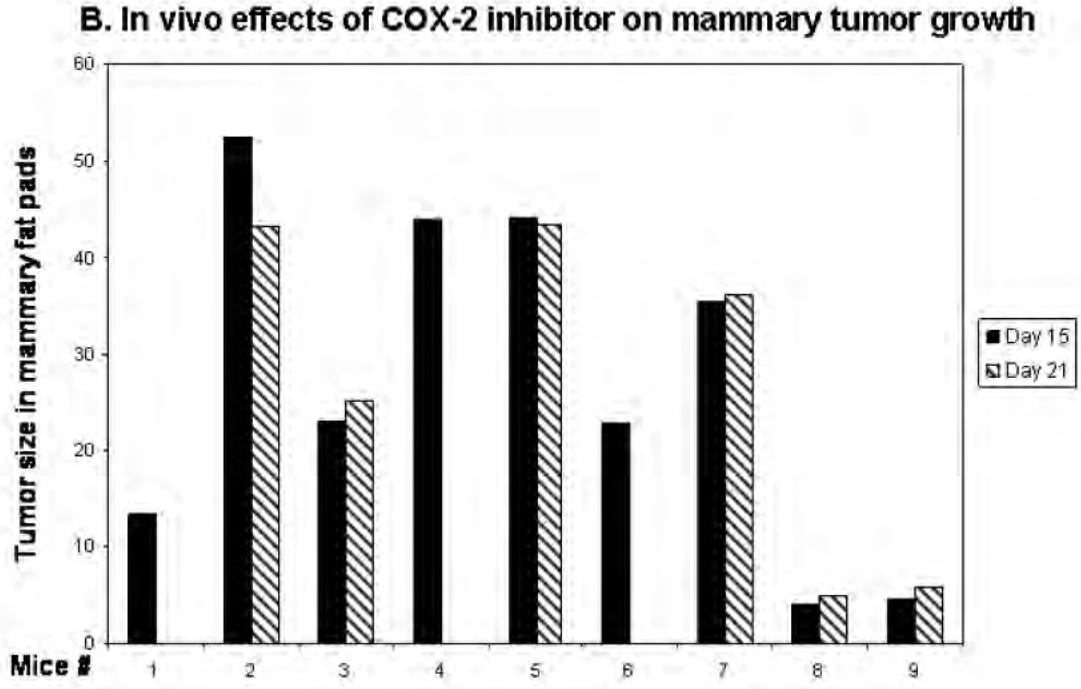
B. In vivo effects of COX-2 inhibitor on mammary tumor growth
Tumor size in mammary fat pads
60
50
40
30
20
10
0
Mice #
1
2
3
4
5
6
7
8
9
Day 15
Day 21

TABLE 5

Figure 1

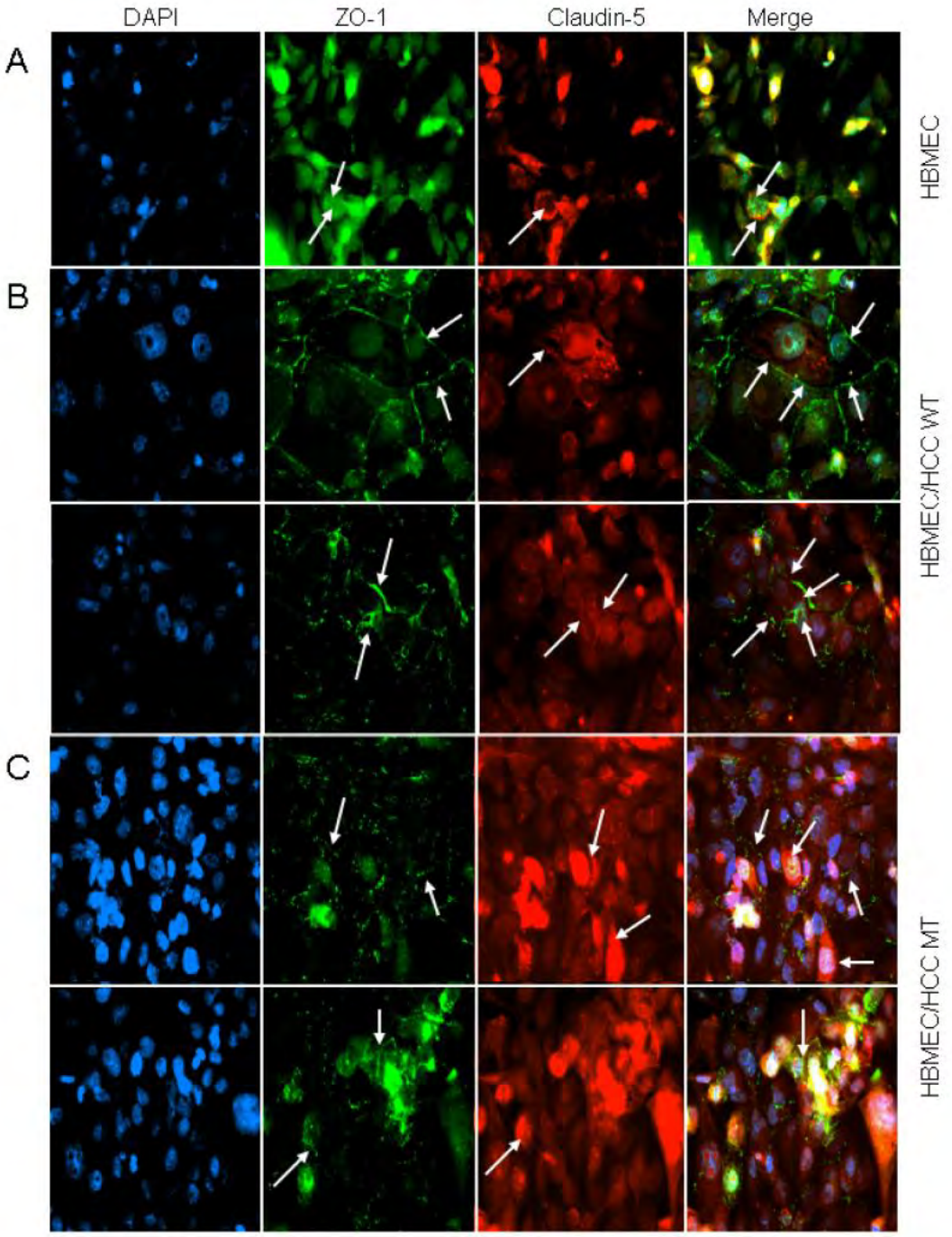

Figure 2

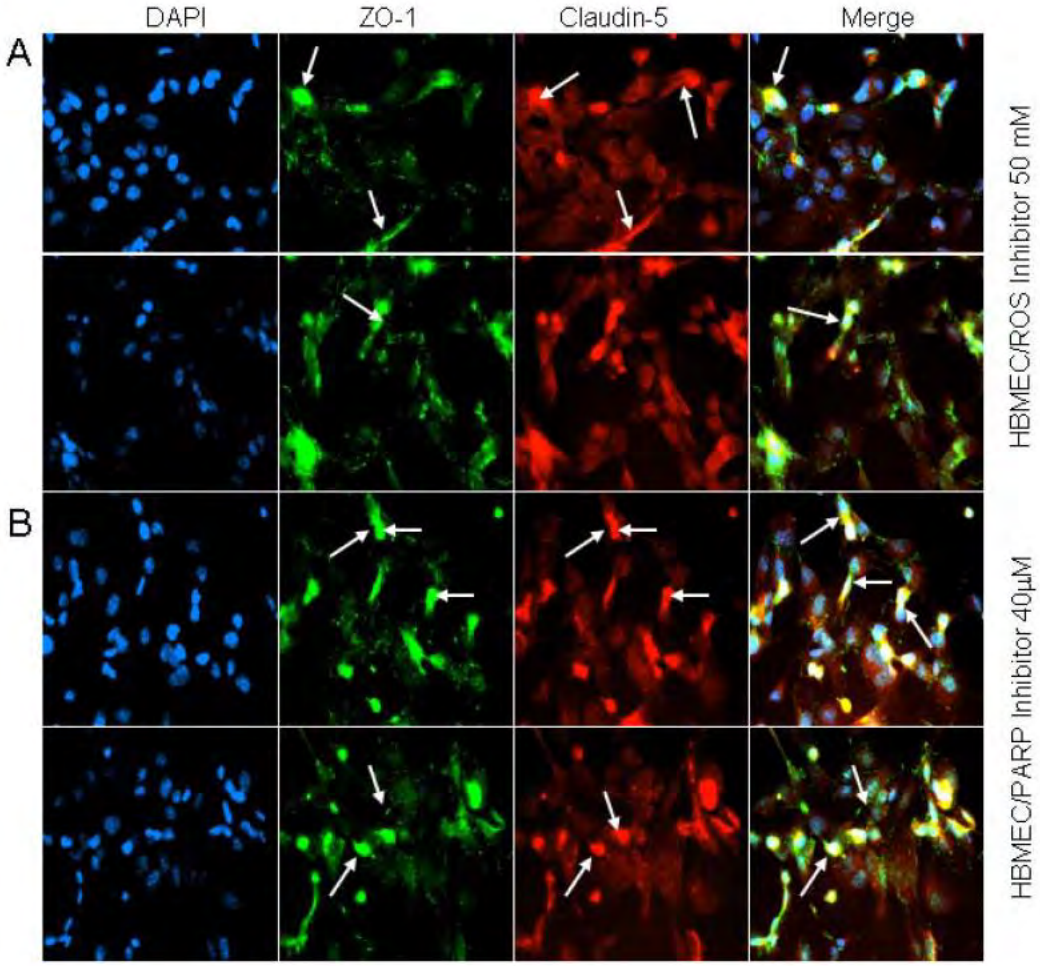
DAPI
ZO-1
Claudin-5
Merge
A
B
HBMEC/ROS Inhibitor 50 mM
HBMEC/PARP Inhibitor 40μM

Figure 3

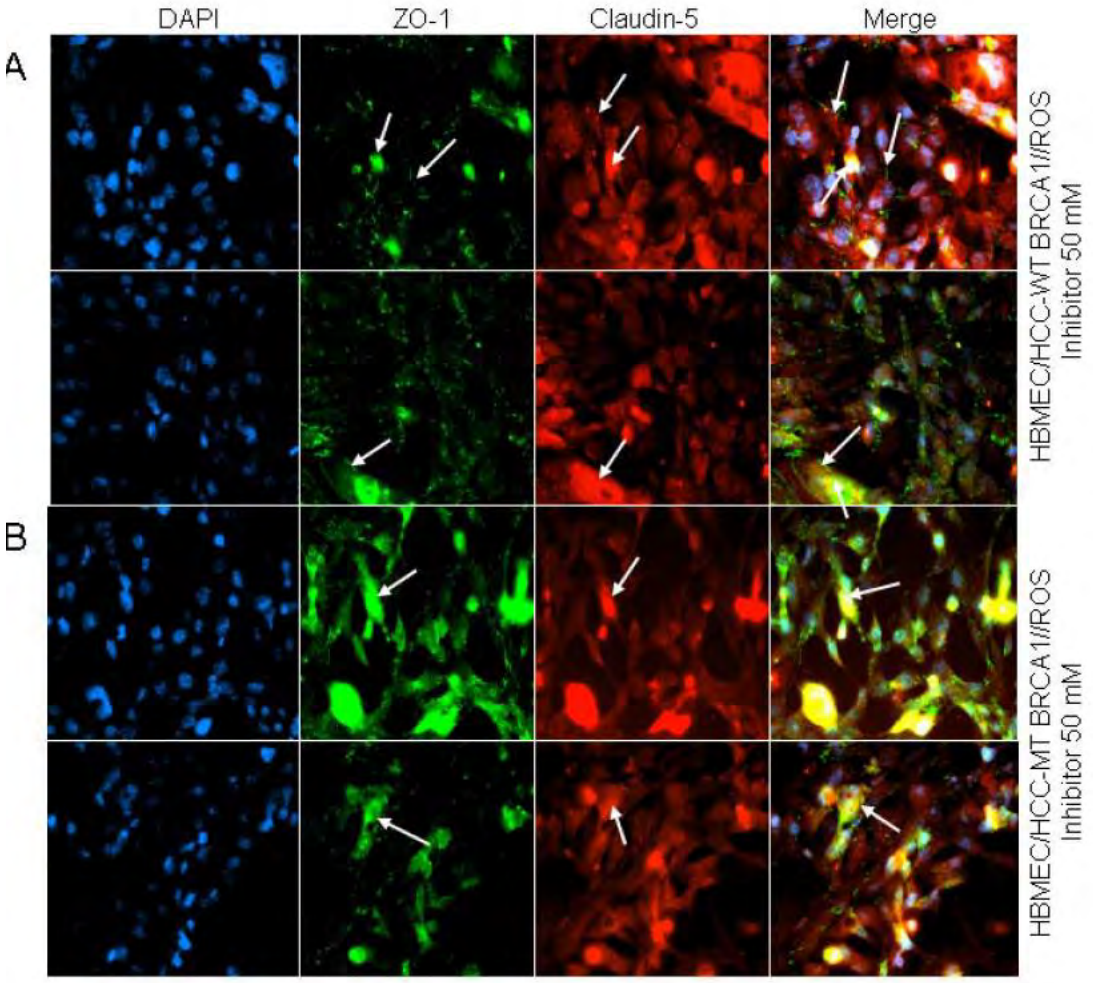
DAPI
ZO-1
Claudin-5
Merge
A
B
HBMEC/HCC-WT BRCA1//ROS
Inhibitor 50 mM
HBMEC/HCC-MT BRCA1//ROS
Inhibitor 50 mM

Figure 4

4A: HBMECs

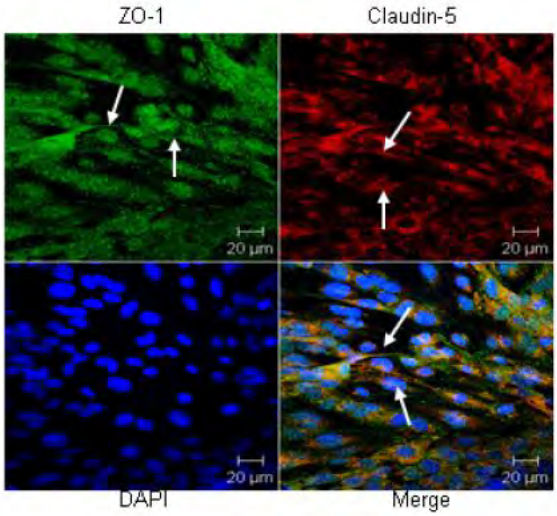

4B: HBMEC / HCC-BRCA1 WT

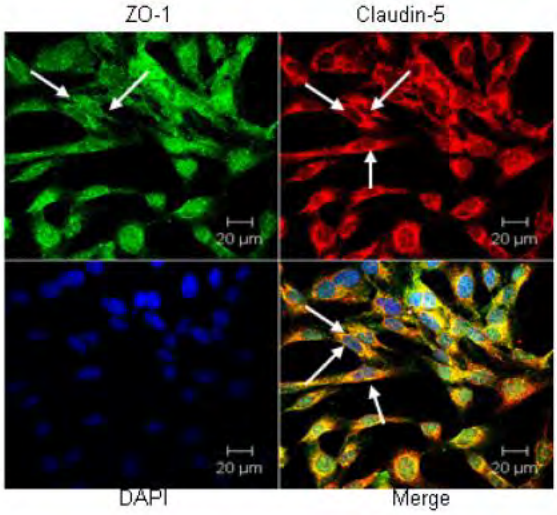

4C: HBMEC / HCC-BRCA1 WT / COX-2 inhibitor

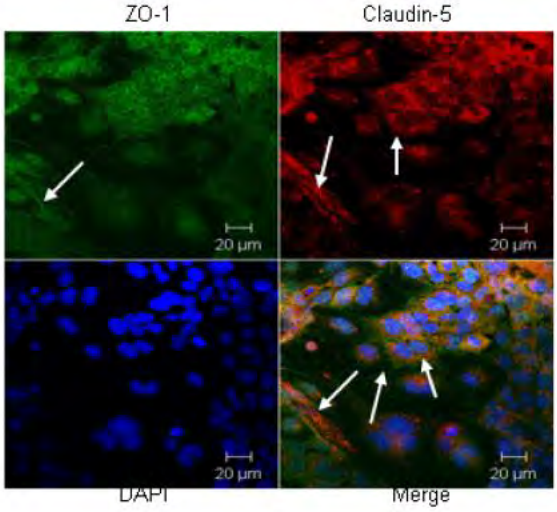

Figure 5

5A. COX-2 RT-PCR

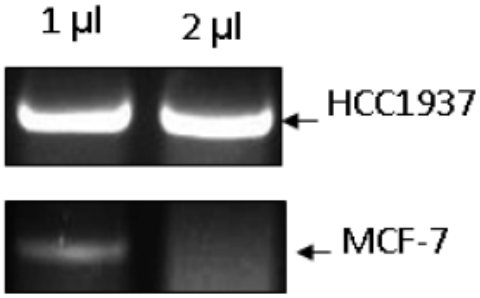

5B. Western blot analysis of COX-2 expression in HCC1937/MT-BRCA1 and HCC1937/WT-BRCA1

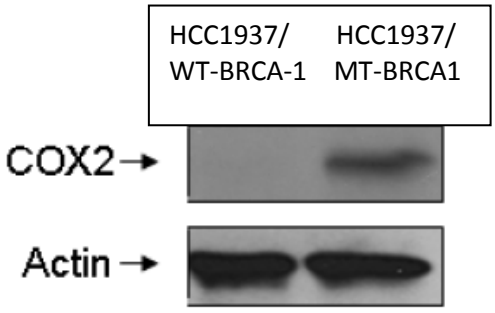

Figure 6

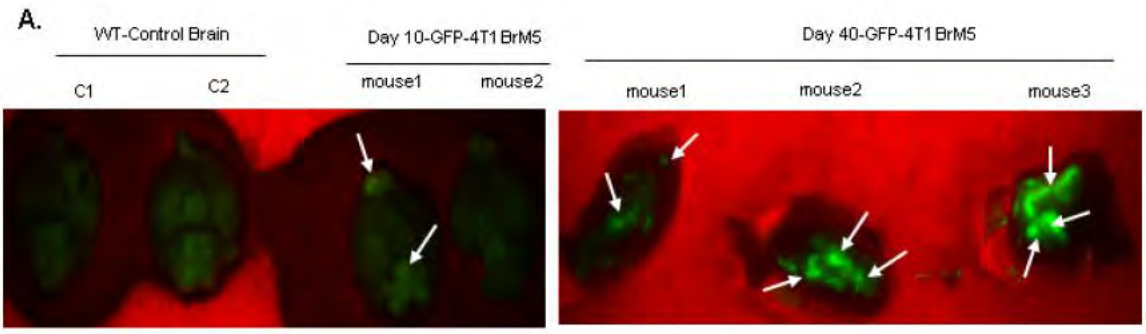
A.
WT-Control Brain
C1
C2
Day 10-GFP-4T1 BrM5
mouse1
mouse2
Day 40-GFP-4T1 BrM5
mouse1
mouse2
mouse3

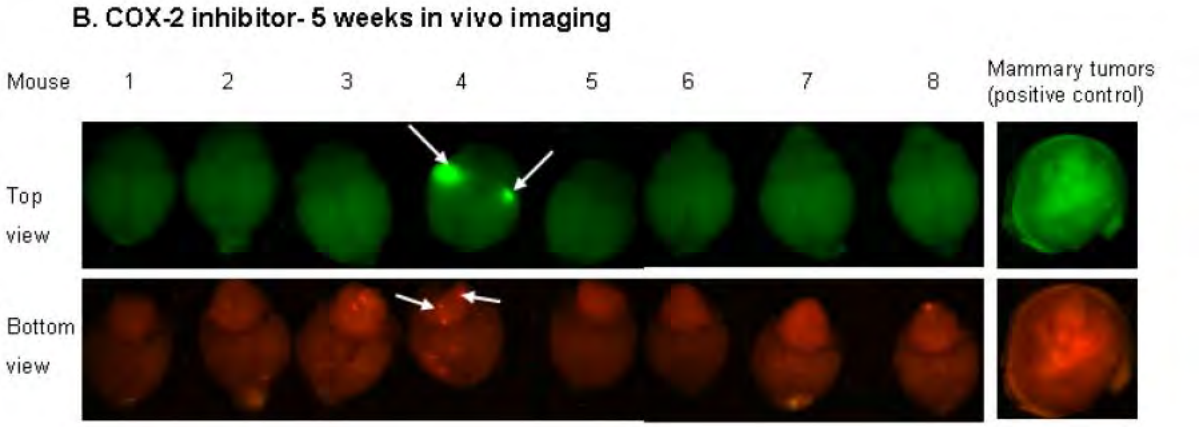
B. COX-2 inhibitor- 5 weeks in vivo imaging
Mouse
1
2
3
4
5
6
7
8
Mammary tumors (positive control)
Top view
Bottom view

Year 3 (No Cost Extension)

No data generated

Key research accomplishments

1) Adhesion to HBMECs by tumor cells expressing mutated BRCA1, as compared to WT BRCA1, is significantly increased and is mediated by ROS production by tumor cells, resulting in alteration of HBMEC permeability.
2) Transmigration of HCC-1937 expressing mutant BRCA1 is enhanced, as compared to tumor cells expressing WT BRCA1.
3) Permeability changes in HBMECs are more pronounced in the presence of MT BRCA, as compared to WT BRCA and these changes can be inhibited by ROS and PARP inhibitors.
4) *In vivo* results showed that COX-2 inhibitors may be viable therapeutic approaches for inhibiting metastasis to the brain in BRCA1 mutated breast cancers.

Reportable outcomes

A manuscript is in preparation.

Conclusion

COX-2 inhibitors may be viable therapeutic approaches in addition to chemotherapy. In addition, they may minimize the risk for breast cancer metastasis to the brain in patients with mutated BRCA1.